Journal of Hazardous Materials 458 (2023) 131899

Contents lists available at ScienceDirect

Journal of Hazardous Materials

journal homepage: www.elsevier.com/locate/jhazmat

The release of polylactic acid nanoplastics (PLA-NPLs) from commercial teabags. Obtention, characterization, and hazard effects of true-to-life PLA-NPLs

Gooya Banaei [a,1], Alba García-Rodríguez [a,1], Alireza Tavakolpournegari [a], Juan Martín-Pérez [a], Aliro Villacorta [a,b], Ricard Marcos [a,*], Alba Hernández [a,*]

[a] Group of Mutagenesis, Department of Genetics and Microbiology, Faculty of Biosciences, Universitat Autònoma de Barcelona, Cerdanyola del Vallès, Spain
[b] Facultad de Recursos Naturales Renovables, Universidad Arturo Prat, Iquique, Chile

HIGHLIGHTS

- Nanoplastics (~116 nm) were obtained from teabags during a standard preparation.
- The FTIR analyses demonstrated that were constituted by polylactic acid.
- Our estimative quantification gives a release of about 1 M PLA-NPLs/teabag.
- High uptake ratios in undifferentiated cells and in Caco-2/HT29 barrier were observed.
- No PLA-NPLs cytotoxicity but a slight barrier disruption could be detected.

GRAPHICAL ABSTRACT

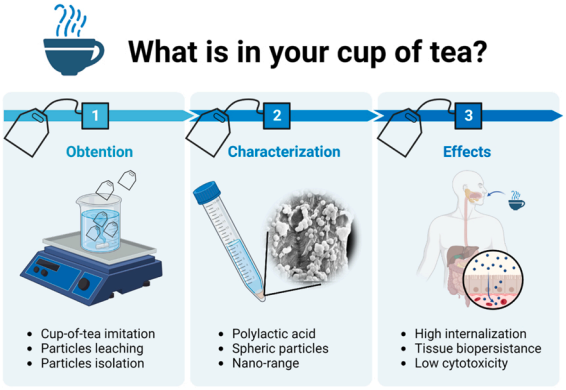

ARTICLE INFO

Editor: Joao Pinto da Costa

Keywords:
Nanoplastics
Teabags
Polylactic acid
Gastrointestinal tract
Food contaminants

ABSTRACT

This study investigates MNPLs release from commercially available teabags and their effects on both undifferentiated monocultures of Caco-2 and HT29 and in the *in vitro* model of the intestinal Caco-2/HT29 barrier. Teabags were subjected to mechanical and thermodynamic forces simulating the preparation of a cup of tea. The obtained dispersions were characterized using TEM, SEM, DLS, LDV, NTA, and FTIR. Results confirmed that particles were in the nano-range, constituted by polylactic acid (PLA-NPLs), and about one million of PLA-NPLs per teabag were quantified. PLA-NPLs internalization, cytotoxicity, intracellular reactive oxygen species induction, as well as structural and functional changes in the barrier were assessed. Results show that PLA-NPLs present high uptake rates, especially in mucus-secretor cells, and bio-persisted in the tissue after 72 h of exposure. Although no significant cytotoxicity was observed after the exposure to 100 μg/mL PLA-NPLs during 48 h, a slight barrier disruption could be detected at short-time periods. The present work reveals new insights into the safety of polymer-based teabags, the behavior of true-to-life MNPLs in the human body, as well as new questions

* Corresponding authors.
E-mail addresses: ricard.marcos@uab.cat (R. Marcos), alba.hernandez@uab.cat (A. Hernández).
[1] Both authors contributed equally.

https://doi.org/10.1016/j.jhazmat.2023.131899
Received 26 April 2023; Received in revised form 30 May 2023; Accepted 18 June 2023
Available online 20 June 2023

on how repeated and prolonged exposures could affect the structure and function of the human intestinal epithelium.

1. Introduction

Micro and nanoplastics (MNPLs) are considered emergent environmental pollutants, due to their wide presence in all the environmental compartments and to the lack of contrasted information on their potential health effects on humans [11]. Human exposure to MNPLs can result from different sources and, possibly, the most important is their environmental presence because of plastic waste degradation. This is assumed because the secondary MNPL composition matches the composition of the original plastic waste [30]. The presence of MNPLs tailored at these ranges (primary MNPLs) is also another important source, mainly associated with the production of cosmetics such as scrub and exfoliating products, and cleaning products [46]. Finally, another relevant source of MNPL exposure results from the migration of MNPLs from food packaging [35]. At this point, special attention should be paid to the release of MNPLs from the herbal/teabags, since during the soaking and steering processes, some MNPLs inevitably detach and migrate to the water solution [2].

In the pioneering study of Hernández et al. (2019) authors stated provocatively that, approximately, 11.6 billion microplastics and 3.1 billion nanoplastics were detected in a single cup of beverage. Using Fourier-transform infrared spectroscopy and X-ray photoelectron spectroscopy the authors demonstrated that the composition of the released particles matched the original teabag materials (nylon and polyethylene terephthalate). In another study, three commercially available filter bags were used to detect the potential release of MNPLs after soaking. Interestingly the nature of the plastic-based food filter bags, measured by Raman imaging combined with chemometrics, were polyethylene terephthalate, polypropylene, nylon 6, and polyethylene [28]. The presence of MNPLs from the breakdown of polyethylene rice cooking bags, ice-cube bags, and nylon teabags has also been demonstrated by using a multi-instrumental approach (Raman microscopy, X-ray photoelectron spectroscopy, and scanning electron microscopy) [7]. Interestingly, the authors proposed to identify the MNPLs release by mass quantification, resulting in 1.13 ± 0.07 mg of nylon 6 from each one of the teabags. Different methods have been applied to detect the release of MNPLs from nylon teabags [24] and polyamide teabags [18]. However, to date, no studies have been found investigating the potentially hazardous effects of those teabags-derived MNPLs.

Aiming to go deeper into the detection of MNPLs resulting from commercially available teabags, we have demonstrated that, contrary to the polymers used in the previously reported studies, the selected brand was constituted by polylactic acid (PLA). This is likely the most popular bio-based polymer, being a biodegradable hydrolysable aliphatic semicrystalline polyester produced through the direct condensation reaction of its monomer, lactic acid, as the oligomer, and followed by ring-opening polymerization of the cyclic lactide dimer [6]. In fact, PLA was observed in one of the three different types of commercial plastic teabags bought from grocery stores in Taipei, Taiwan. The other two types were determined as PE/PET and PET, respectively [9].

It should be remembered that PLA has gained popularity in the food industry due to its many advantages, which have been described to be (i) *eco-friendly* since it is a plant-based polymer, and can be recyclable and compostable, (ii) *biocompatible* as no toxic effects have been reported and (iii) *economically competitive* since PLA required up to 55% less energy to produce than petroleum-based polymers [36]. However, it has been extensively reported that not all plant-based polymers (*e.g.,* PLA) biodegrade as ideally in the environment. A recent study stated that teabags made of PLA bio-persisted completely intact in soil throughout all the time points (up to 12 months) [26]. Thus, together with petroleum-based polymers, PLA contributes to overall plastic contamination and there is of an urgent need to address their potential effects on human health. To such end, in addition to a complete physicochemical characterization of the released PLA-MNPLs from teabags, the present study has evaluated the fate and bio-interactions of ingested teabag-derived PLA-NPLs as well as their effects using the *in vitro* model of the human intestinal barrier constituted by Caco-2/HT29 cocultures. Accordingly, this is the first approach aiming to determine *in vitro* the potential hazards posed by true-to-life NPLs released from PLA plastic teabags.

2. Materials and methods

2.1. PLA nanoplastics obtention

A brand of commercially available teabags from the local market was purchased in a box format containing 50 teabags each. To obtain particles from the teabags' filters, the protocol described in Fig. 1 was followed. This protocol tries to mimic a traditional cup-of-tea preparation procedure. First, each teabag was individually opened/unfolded, emptied by hand (the tea discarded), and carefully washed 3 times with Milli-Q water. A total of 300 teabags were dropped into a 1 L beaker (prewashed and autoclaved-sterilized) containing 600 mL of Milli-Q water preheated at 95 ºC under constant stirring. The stirring speed was gradually augmented since the weight of the teabags slowed down the stirring speed, and the final setting was set up to 750 rpm. Next, the teabags were squeezed to mimic a realistic cup-of-tea procedure and eliminated from the aqueous solution for any future step. The remaining solution was left to cool down on constant stirring and the volume was ultracentrifuged to spin down the released content by ultracentrifugation (25 min at 13 200x g). The supernatant was discarded, and 1 mL of sterile Milli-Q water was transferred, tube by tube (if the sample was ultracentrifuged in several tubes depending on the ultracentrifuge capacity), to collect and concentrate the teabaǵs derived pellet by second ultracentrifugation. Once the supernatant was eliminated, ethanol (1 mL) was carefully added to sterilize the sample. Finally, the pellet was let to dry overnight under sterile conditions. The remaining dried and sterilized pellet in the tube was weighed 3 times to determine the concentration of isolated particles [15 mL tubes containing teabags-derived pellet – empty 15 mL tubes = weight of the teabags-derived pellet].

The use of 300 teabags simultaneously in 600 mL was found to yield enough amount of particulate material (~ 6000 μg) which reached the concentration limits to perform a proper particle characterization as well as further biological experiments without compromising the osmolarity of the cell culture medium.

2.2. PLA nanoplastics characterization

The PLA nanoplastics obtained as above indicated were characterized under three different conditions, (1) right after the particles' isolation, (2) after dispersion following the Nanogenotox dispersion protocol [31], and (3) after the dispersed particles were diluted in DMEM culture medium containing 10% FBS. The three different states were named (1) non-sonicated, (2) sonicated, and (3) culture medium. Only the sonicated particles diluted in DMEM were used to expose the cells. Different approaches were used for PLA nanoplastic characterization as indicated below.

2.3. Scanning electron microscopy (SEM) to visualize teabag surfaces and dispersions

Teabags' surface morphology was visualized by scanning electron

microscopy (SEM) (Zeiss Merlin, Zeiss, Oberkochen, Germany). Briefly, tiny pieces of teabags were cut and pasted using conductive carbon adhesive tape (Agar Scientific, Ltd., UK). Then, several representative images were taken from a random field of view. For the shape description of PLA nanoplastics in dispersion (non-sonicated, sonicated, and diluted in DMEM) 10–20 μL drops were deposited in a carbon-coated tab (Agar Scientific, Ltd., UK) and left to dry before imaging.

2.4. Particles' shape analysis with transmission electron microscopy (TEM)

TEM was used to visualize the particle's shape as well as the primary particle diameter. Briefly, after the PLA-NPLs isolation from the teabags, a copper grid covered with carbon film was dipped into the particle's stock dispersion (200 μg/mL). The soaked grids were allowed to dry overnight, and the particles entrapped in the carbon-coating of the grid were examined with a JEOL JEM 1400 instrument (JEOL LTD, Tokyo, Japan). Several pictures were randomly selected. Later, TEM images were analysed for particle size distribution using the ImageJ software 1.8.0_172 and processed with the GraphPad Prism 7.0 software.

2.5. Chemical identification using Fourier Transform Infrared Spectroscopy (FTIR)

FTIR was used to identify the type of polymer associated with our sample. This technique is suitable for quickly identifying compounds such as plastics, resins, coatings, blends, and paints among others. Briefly, a drop of the teabags' isolated particles (non-sonicated) was deposited on a fold mirror and left to dry for seven days under sterile conditions. The further steps used a Vertex 80 device (Bruker Corporation, Billerica, Massachusetts, USA). Interferograms were analysed to identify the peaks corresponding to the polymer of interest.

2.6. Hydrodynamic size determination by using Dynamic light scattering (DLS) and laser Doppler velocimetry (LDV)

DLS and LDV were used to determine the hydrodynamic size, polydispersity, and zeta potential of PLA nanoplastics when dispersed in all three stages (non-sonicated, sonicated, and diluted in DMEM). Briefly, 1 mL of particle suspension at a concentration of 100 μg/mL was injected into capillary cells with fold-plated beryllium-copper electrodes (DTS1070), previously rinsed with sterile Milli-Q water to avoid potential dust contamination. The refractive index used to measure PLA particles was 1.476. Samples were equilibrated for 120 s at 25 °C in the instrument chamber, before the measurement with a Malvern Zetasizer Nano Zs zen3600 device (Malvern Panalytical Ltd., UK).

2.7. Quantification of the released nanoparticles by nanoparticle tracking analysis (NTA)

The number of particles released in the aqueous media before and after the sonication was measured for nanoparticle tracking analysis with a Nanosight NS300 (Malvern Panalytical Ltd., UK) and NTA software version 3.4. As in DLS, NTA uses both light scattering and Brownian motion to detect particles and obtain their size distribution and concentration in liquid suspensions. Briefly, at least 1 mL of non-sonicated and sonicated dispersions (100 μg/mL) were injected into the Nanosight using a 2 mL syringe pump at a speed of 50 AU and detected using a blue laser (488 nm) and a camera-type sCMOS.

2.8. Cell culture conditions, in vitro model development, and exposure to PLA-NPLs

Two different cell lines derived from colon adenocarcinomas, namely Caco-2 and HT29, were used as both (i) undifferentiated monoculture and (ii) differentiated co-cultured conditions. The main differences between undifferentiated and differentiated cultures are the cell complexity degree and barrier-like structure. While differentiated cells show a higher level of cellular complexity along the culture days, with Caco-2 developing into a polarized columnar cell type (enterocyte-like cells) containing microvilli and tight junctions and HT29 producing an extracellular mucus layer (goblet-like cells), the undifferentiated cells do not have the time to develop those cell traits since are only left growing for 1 day.

Caco-2 cells were originally supplied by Dr. Isabella de Angelis (ISS, Italy). The HT29 cell line was from the American Type Culture Collection (ATCC, Manassas VA, USA). The two cell lines were maintained in Dulbecco's modified Eagle's High Glucose medium (DMEM) without sodium pyruvate supplemented with 10% fetal bovine serum (FBS), 1% non-essential amino acids (NEAA), 1% Amphotericin B (Biowest, France), and 2.5 μg/mL Plasmocin (Invivo Gen, San Diego, CA). Cells were cultured in T75 cm^2 flasks in a humidified atmosphere of 5% CO_2 and 95% air at 37 °C. Both cells were subcultured weekly when arriving at 70–80% of confluency, dispersing them with 1% trypsin-EDTA (Biowest, France).

For experiments using undifferentiated cells, both Caco-2 and HT29 were seeded individually in 12 well plates at 1.7×10^5 cells/well and left to attach for 24 h. After 24 h cells were exposed to the teabags-derived PLA-NPLs (0, 50, and 100 μg/mL) for at least 48 h.

For the *in vitro* barriers (Caco-2/HT29) formation and differentiation, a total of 1.7×10^5 cells were seeded on 1.12 cm^2 PET Transwell® containing pores of 1 μm (Merck KGaA, Darmstadt, Germany). Briefly, Caco-2 and HT29 cells were co-cultured for 21 d at a ratio of 90/10 to obtain a well-differentiated and polarized barrier as previously described [19,20]. The culture medium was changed every 2 d. After the differentiation period (21 d), the *in vitro* barriers were exposed to

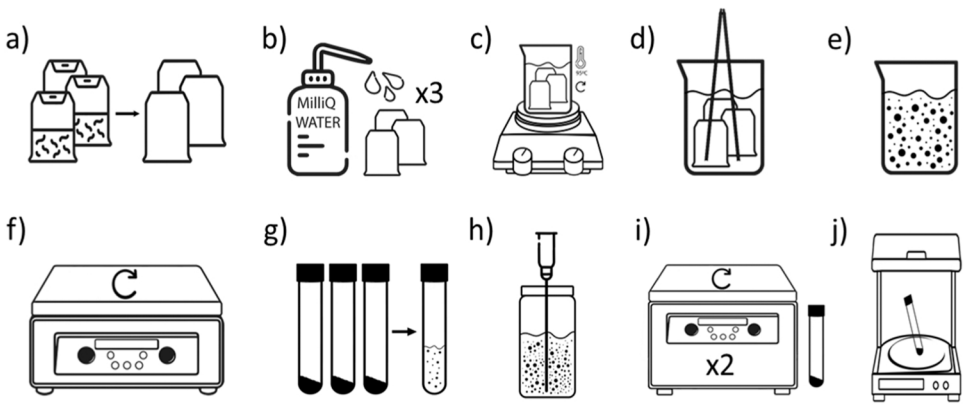

Fig. 1. Schematic representation of the isolation of nanoplastics derived from PLA teabags. (a) Open the filter bags and discard the tea. (b) Wash with sterile Milli-Q water to remove tea leftovers. (c) Boil (95 °C) sample in sterile Milli-Q water while stirring (750 rpm). (d) Squeeze and remove teabags with a glass sterile chopstick. (e) The remaining suspension of particles in the aqueous solution. (f) Ultracentrifugation of the whole sample volume using different tubes. (g) Supernatant removal and pellet resuspension and concentration. (h) Total pellet ultracentrifugation, sterilization, and evaporation. (I and j) After new centrifugations, the sterilized and dried pellet was weighted.

teabags-derived PLA-NPLs (0, 50, and 100 μg/mL or 0, 2.475 $\times 10^{10}$, 4.95 $\times 10^{10}$ particles/transwell) for at least 72 h (Calculations are disclosed in Supplementary Materials). The concentrations of PLA-NPLs used for the *in vitro* studies were found to be subtoxic (Fig. 1 in Supplementary Material) and suitable for tracking the particles under the confocal microscope; however, these concentrations do not relate with those found in the characterization studies and are not intended to be physiologically relevant.

2.9. Cell internalization by confocal microscopy

To visualize the fate of the teabags-derived NPLs in both undifferentiated cells and differentiated *in vitro* barrier, confocal laser microscopy was used. To such end, NPLs were labeled with iDye Poly Pink (a dye well-known to color polymers) before treating the cells [38]. Briefly, undifferentiated Caco-2, undifferentiated HT29, as well as the differentiated *in vitro* barrier Caco-2/HT29 were exposed to labeled PLA-NPLs (100 μg/mL) for 24, 48, and 72 h, respectively. After the treatment, cells were washed twice with PBS 1x and live stained with Hoechst 33342 (1:500 in DMEM) and CellMask™ Plasma Membrane Stains (1:500 in DMEM) (Termo Fisher Scientific Inc., USA) for 15 min to stain the cell nucleus and membrane, respectively. The transwell membranes were cut, placed in a microscope slide, mounted with DMEM, and covered with a cover slide for immediate imaging. Confocal images were acquired with a Leica TCS SP5 confocal microscope (Leica, Germany). ImageJ was used to analyse and process the obtained images.

2.10. Internalization studies by flow cytometry

To determine and quantify the percentage of living cells containing labeled PLA-NPLs (attached or internalized) a BD-FACSCanto Flow Cytometer (BD Bioscience, USA) was used. Briefly, after the exposure to 100 μg/mL iDye-labeled NPLs cells were washed twice with PBS 1x, trypsinized, and resuspended in PBS 1x to obtain 1×10^6 cells/mL. Samples were kept on ice before sample analysis. At least 10,000 events were counted per sample.

2.11. Detection of intracellular reactive oxygen species (ROS)

The dihydroethidium (DHE) assay kit (Abcam plc.) was used to analyse the ROS levels on the *in vitro* barrier constituted by Caco-2/HT29 cells. After the exposures to 0, 50, and 100 μg/mL of teabags-derived PLA-NPLs for 3, 24, and 48 h, barriers were washed twice with PBS 1x, trypsinized, resuspended in PBS 1x containing 10 μM DHE to a final concentration of 1×10^6 cells/mL and incubated for 30 min at 37 °C. After incubation, the excess DHE was removed by centrifugation, cells were resuspended in PBS 1x and kept on ice. Before the analysis, and to determine cell viability, samples were incubated with 3 nM VPR (Via-ProbeTM Red Nucleic Acid Stain, BD Bioscience, USA) for 5 min. At least 20,000 events were analysed from the living-cell population using a BD-FACSCanto Flow Cytometer (BD Bioscience, USA). As a positive control, samples exposed for 45 min to 100 μM Antimycin A (AMA) were used.

2.12. Evaluation of the barrier's integrity and permeability

The transepithelial electrical resistance (TEER) was assessed to determine the integrity of the *in vitro* barrier, using an epithelial voltmeter, Millicell-ERS volt/Ohm meter (Merck KGaA, Darmstadt, Germany). Briefly, the *in vitro* barriers were exposed to 0, 50, and 100 μg/mL of teabags-derived PLA-NPLs for up to 48 h. Every 24 h, the treatments were removed, the barrier was washed with PBS 1x, and fresh DMEM was added in the apical and basolateral compartments. For each sample, two different parts of the insert were selected for measurements.

On the other hand, the Lucifer yellow (LY) assay (ThermoFisher Scientific, USA) was used to evaluate the barrier's permeability after exposing the *in vitro* barriers to the previously mentioned treatments. Briefly, treatments were removed, and the barriers were washed (apical and basolateral compartment) thrice with Hank's balanced salt solution (HBSS, Sigma-Aldrich, Germany). Then, transwells® were transferred to a new 12-well plate, each well containing 1.5 mL of HBSS in the basolateral compartment and 0.5 mL containing 0.4 mg/mL of LY diluted in HBSS was added to the apical side. After 2 h of incubation at 37 °C, for each sample, 100 μL of the basolateral content was transferred twice to a black 96 well-plate to measure the passage of LY. LY is able to cross cell barriers only *via* the paracellular route, which makes it suitable for analyse of changes in barrier permeability. Samples were measured with a fluorimeter (Victor III, Perkin Elmer, USA) using an excitation-emission spectrum of 405–535 nm. As a positive control, cell-free inserts were used.

2.13. Statistical analysis

All the experiments were carried out in at least two different biological replicates, containing at least three replicates per treatment. Results are expressed as mean ± standard error (SE) or mean ± standard error of the mean (SEM). First, data were analysed with the two most recommended normality tests to determine the Gaussian distribution of the values. Hence, both D'Agostino-Pearson omnibus normality and Shapiro-Wilk normality tests were determined using GraphPad Prism version 9. After passing the normality test, one-way or two-way ANOVA followed by Tukey's or Dunnet's post-tests were used to compare differences between means. All data were analysed with GraphPad Prism Version 9.00 for Windows (GraphPad Software, San Diego California, USA). Differences between means were considered statistically significant at $P < 0.05$.

3. Results and discussion

3.1. Characterization of teabags filters

The commercially available used teabags were subjected to a deep characterization by SEM. Fig. 2A shows the original teabag shape without the tea leaves. Smaller pieces of those filters (about 3 cm^2) were used to closely visualize their morphology by SEM. Thus, Figs. 2B, and 2C show the fibers constituting the teabag which has an amorphous or even a flaky surface, which can potentially lead to particle leaching when thermal, mechanical, or even chemical stress is applied. Spherical bodies in the nano range were also seen attached to the fibers (Fig. 2D). Similar results were observed by other authors who reported small particles on the filter fibers which disappeared when the samples were steeped at 95 °C or soaked in water [23,28].

3.2. Characterization of the released particles

When simulating a cup-of-tea preparation, all the above-mentioned stressors are present: boiling, stirring, and squeezing, in addition to the presence of water and additives. Hence, after subjecting the teabags to the simulation represented in Fig. 1, a deep characterization of the released and/or leached content into the aqueous media was performed. Since the aim of this study was to use the teabags-derived particles for toxicological *in vitro* studies, the released content was characterized in three different conditions: (i) immediately after the cup-of-tea simulation (non-sonicated in water), (ii) after being dispersed using the Nanogenotox dispersion protocol (sonicated + water), and (iii) after the dispersion and dilution in complete cell culture medium (sonicated + DMEM+10% FBS). TEM and SEM images depicted in Fig. 3 show the presence of spherical particles present in the aqueous solution released/leached from the boiling, steering, and squeezing steps (Fig. 3.A.1 and 2). The primary particle size was calculated to be around 160 nm, and after its dispersion by sonication, the size diminished up to 114 nm. However, its dispersion in the complete culture medium did not affect

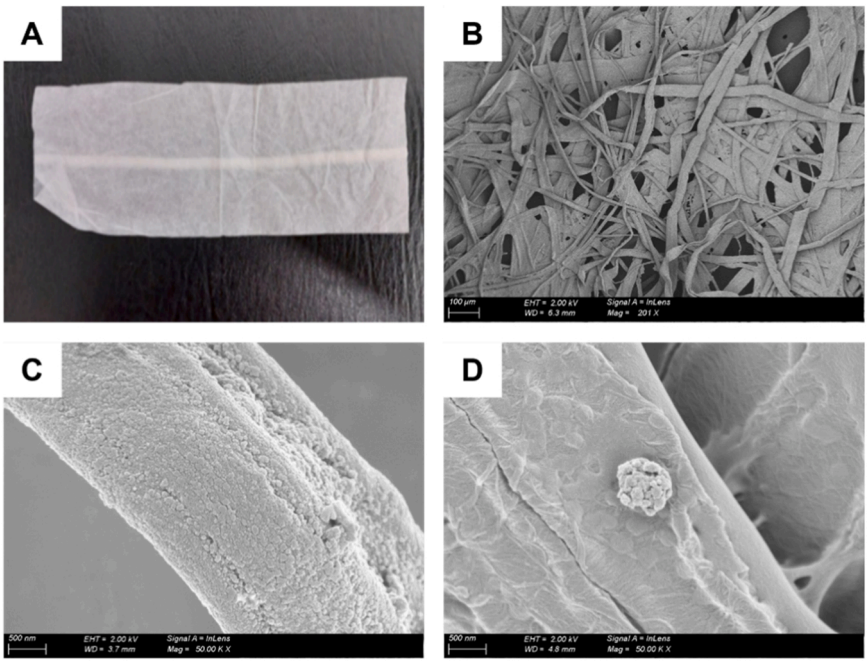

Fig. 2. Teabag's filter analysis by SEM. (A) Picture of an original emptied teabag. (B) SEM image of a teabag piece at low magnification. (C and D) SEM image of a single fiber surface.

the particle diameter. A tendency of particles deagglomeration can be observed by looking at the SEM images, as the particles in panel A.2 (non-sonicated sample) are seen agglomerated while particles in panel B.2 (sonicated) and B.3 (sonicated+DMEM+10% FBS) are more individualized. This trend is corroborated by the DLS results since the hydrodynamic size of the non-sonicated samples is much higher (~400 nm) than the sonicated with (~280 nm) or without DMEM (~270 nm). The Zeta potential measured by DLS showed that, in water, the extracted particles are negatively charged (−34.30 ± 2.52 mV), but the charge diminished –reaching a neutral state– when the particles were diluted in DMEM+ 10% FBS (−5.95 ± 1.88 mV). The NTA analysis also detected a reduction in the hydrodynamic size when the teabags-derived NPLs were sonicated (Fig. 3. E). This phenomenon could be explained by the formation of a "bio-corona" where the PLA particles could be "coated" with proteins and other molecules present in the cell culture medium supplemented with 10% FBS, avoiding the formation of ester bound between units of lactic acid. In our previous work studying the effects of oral digestion in polystyrene (PS-NPLs), we already detected the adhesion of proteins in the PS-NPLs' surface which led to a slight reduction of the particle diameter (from 66 to 60 nm) [39]. In the work of Hernandez et al. [23], differences in the leached NPLs were already reported, in which some were detected to be spherical, and others with irregular shapes and agglomerates [23].

Several studies have also reported the release of billions of MNPLs from teabags. Among them, polymers such as nylon, polypropylene, and polyethylene terephthalate were the most detected in commercially available teas [2,23,28].

However, when the suspension of NPLs was analysed by FTIR, the resulting spectrum confirmed the chemical structure of the biodegradable polymer as a polylactic acid (PLA). The IR spectrum of polylactic acid shows a strong band around 1757 cm^{-1} corresponding to C═O bond stretching, and the bands at 2990 cm^{-1} and 2950 cm^{-1} belonging to C-H stretching of -CH_3. Hence, the FTIR spectrum obtained from the particles leached in the aqueous suspension corresponds to the IR spectra of PLA already reported in the literature [8,29].

3.3. Quantification of the teabag leachate particles

As a relevant approach, the number of PLA-NPLs released into the aqueous media was measured using both NTA and DLS methodologies. Fig. 4 shows the histograms of the particle concentration and intensity calculated by NTA (5.20×10^7 particles/mL) and DLS (4.66×10^7 particles/mL), respectively. Thus, an average of 50 million particles per mL were found in the aqueous solution where the teabags were boiled, steered, and squeezed simulating a cup-of-tea preparation. However, if we consider that 300 teabags were boiled in 600 mL, a total of 1×10^8 particles are released from a single teabag (Table S1 of Supplementary Information). Is honest to highlight that, possibly, the use of 300 teabags for its simultaneous particle extraction might substantially influence the number of particles released -most likely due to the abrasion between them.

Unlike all the previous studies, we have considered that in the aqueous solution, there are not only PLA-NPLs but fiber pieces or even carbon nano-dots coming from tea leaves that could not be washed away in previous steps and could be counted as particles during the NTA analysis. Then, considering only the number of particles present in the non-sonicated solution with diameters like the ones obtained by TEM (159.48 nm), DLS (395.09 nm), and NTA (211.80 nm) (±10 nm) separately, the number of particles released per teabags significantly decrease up to 7.86×10^6, 3.45×10^5, and 1.25×10^6, respectively (Table S2 of Supplementary Information). Our results are significantly different compared to those previously reported, which are about two orders of magnitude higher [23,43], although no PLA content was observed in their evaluated teabags. Thus, Hernandez et al. [23] reported finding 2.3 million particles/teabag and 14.7 billion particles/teabag in the micron and submicron range (21% of which are in the nano range), respectively, when imaging dry leachates by SEM. They also used NTA analysis, which tracked an average of 14.3 M submicron particles/teabag (like their SEM results). However, a comment on this work suspected that not all the particles observed were in fact micro- and nanoplastic ranges, since no information on a ratio between plastic and non-plastic particles was given [5]. Based on their experiments, Busse et al. [5] suggested that the particles detected by SEM could be crystallized oligomers since monomers and oligomers from nylon

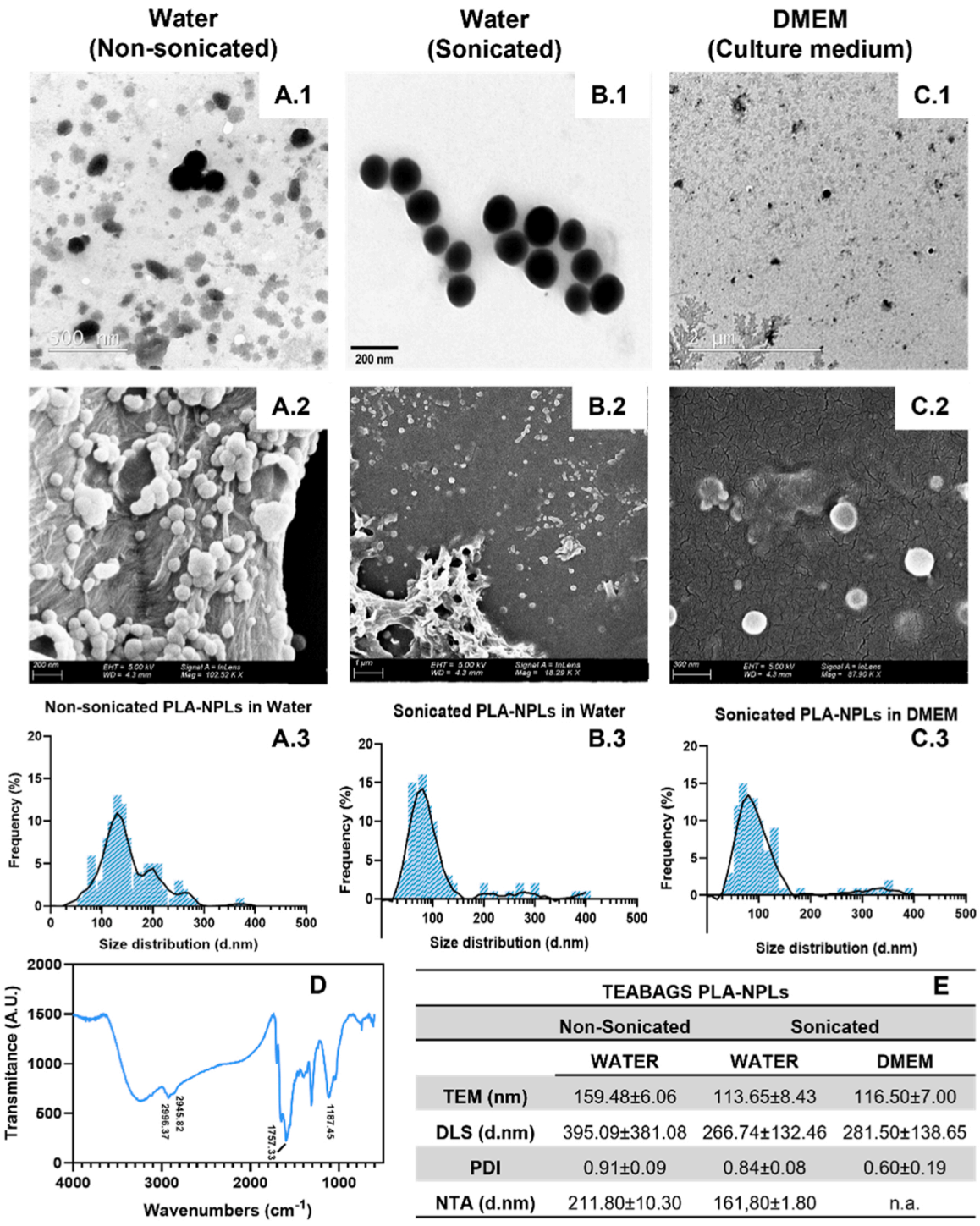

E

TEABAGS PLA-NPLs	Non-Sonicated	Sonicated	
	WATER	WATER	DMEM
TEM (nm)	159.48±6.06	113.65±8.43	116.50±7.00
DLS (d.nm)	395.09±381.08	266.74±132.46	281.50±138.65
PDI	0.91±0.09	0.84±0.08	0.60±0.19
NTA (d.nm)	211.80±10.30	161,80±1.80	n.a.

Fig. 3. PLA-NPLs detection and characterization. (A.1, B.1, and C.1) present TEM images of teabags-derived NPLs (100 µg/mL). (A.2, B.2, and C.2) present SEM images of teabags-derived NPLs (100 µg/mL). (A.3, B.3, and C.3) show the frequency histograms of the primary particle size distribution measured from TEM images. (D) shows the FTIR analysis from a teabag-derived PLA-NPLs suspension. (E) DLS and NTA data.

teabags (93 µg/L caprolactam and 73 µg/L 1,8-diazacyclotetradecane-2, 9-dione) were detected in the medium by LC-MS/MS. Another study based their particle number calculations on the image analysis of microscopic Vis/NIR hyperspectral images at 40x and the FTIR spectral analysis [43]. In that work, the authors estimated that a single teabag produced 1.3 billion nylon microplastic particles and concluded that the number is a wide overestimation since the real particle number is practically unavailable because most of the spherical particles are found either in the form of assemblage or agglomerated. Multiple reasons can be provided discussing the wide differences in particle release between studies. The lack of standardized protocols on particle extraction and isolation, leachate preparations as well as the analytical techniques used to detect and quantify are the main source of variability. Moreover, differences in the particle leaching between teabags may be also explained by differences in the teabag production, teabags contamination, material quality, and polymer characteristics (density, strength, additives, age, *etc.*) as well as the stringency of the surrounding matrix.

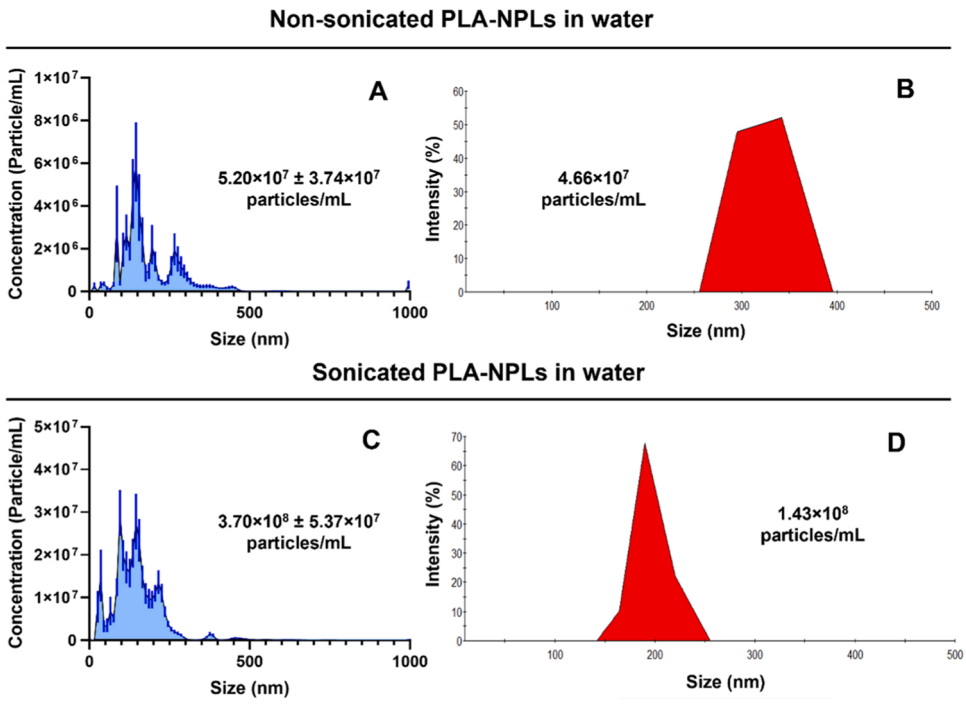

Fig. 4. The number of PLA particles released from teabags. The concentration of PLA particles was measured by NTA (A) right after hot water-steeping 300 teabags in 600 mL and (C) after dispersing the solution by sonication. DLS results on particle intensity and concentration after (B) hot water-steeped teabags and (D) after sonication.

3.4. In vitro fate and bio-interactions of PLA-NPLs

In addition to the physicochemical approaches, this study aimed to determine the potentially hazardous effects of the leached particles from the teabags (PLA-NPLs). Hence, before exposing our *in vitro* models (undifferentiated monocultures of Caco-2 and HT29 and differentiated

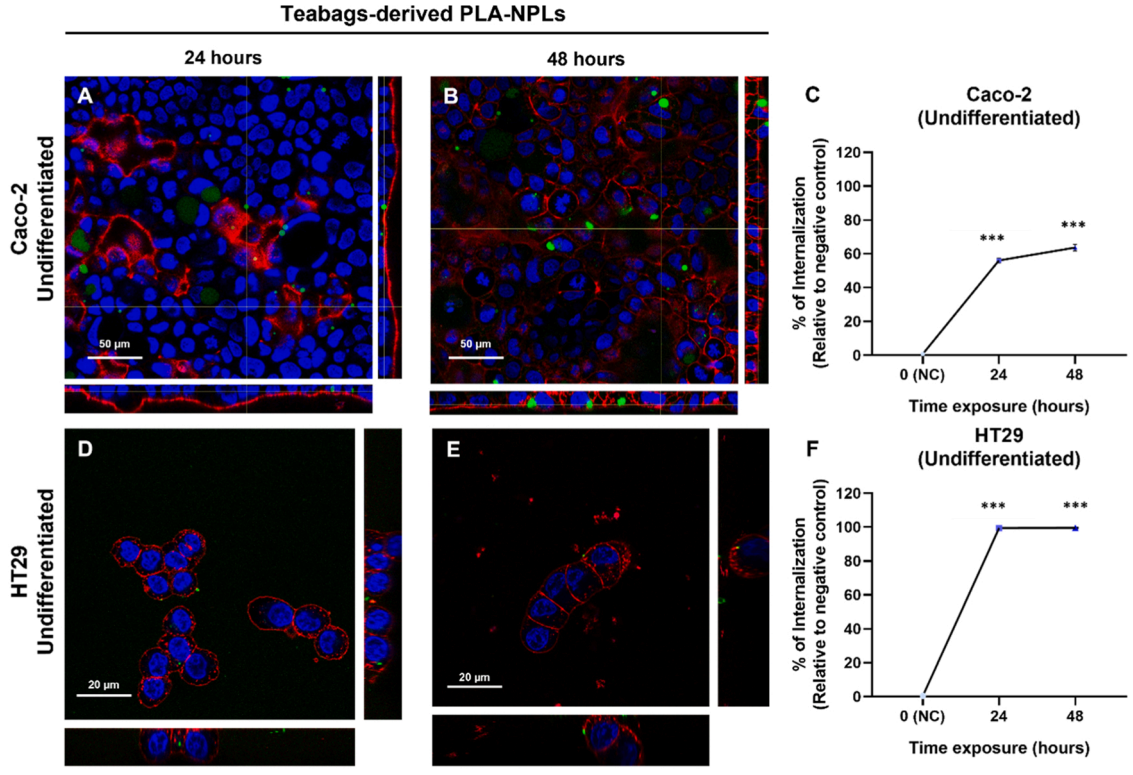

Fig. 5. Teabags-derived PLA-NPLs internalization studies using undifferentiated monocultures. (A and B) Confocal images of Caco-2 cells exposed to 100 µg/mL of PLA-NPLs. (C) Quantification by Flow Cytometry of PLA-NPLs internalization into Caco-2 cells. (D and F) Confocal Images of HT29 cells exposed to 100 µg/mL PLA-NPLs. (F) PLA-NPLs internalization into HT29 cells measured by flow cytometry. PLA-NPLs (green), nuclei (blue), and cell membrane (red) were stained with iDYE, Hoechst 33342, and CellMask™, respectively. Data is represented as mean±SEM and analyzed using one-way ANOVA with Dunett́s post-test. * ** $P < 0.001$.

Caco-2/HT29 coculture barrier) we used a standardized nanoparticles' dispersion protocol to homogenate the solution. As indicated in the previous section, in general, the number of particles present in the aqueous dispersion increased after the sonication suggesting that the dispersion protocol successfully disaggregated the agglomerated NPLs (observed in TEM and SEM images) and, consequently, increased the number of individualized particles.

Firstly, the capability of PLA-NPLs to internalize into cells was assessed in monocultures of both Caco-2 and HT29 cells after exposures lasting for 24 and 48 h. The used cells are colon-derived cells and are the most popular when using *in vitro* experiments. Cell uptake studies by flow cytometry found that while 100% of HT29 cells interacted and/or internalized at least one PLA-NPL, only 60% of Caco-2 cells did it (Fig. 5. C and F). The PLA-NPLs internalization was also corroborated by confocal microscopy. As shown in Fig. 5, fluorescently labeled (iDYE pink) PLA-NPLs (shown in green) were detected mainly in the cell cytoplasm and in some cases interacted with the cell nucleus (blue) of both Caco-2 (panels A and B) and HT29 (panels D and E) cells.

Only a few studies have investigated the cell fate of pristine (free-coating) PLA-NPLs since in biomedicine most of the attention was given to copolymerized PLA such as PEG-PLA (polyethylene glycol-PLA), PLGA (poly lactic-co-glycolic acid), PLA-TPGS (-alpha-tocopheryl polyethylene glycol 1000 succinate), etc, seeking for a better nano-carrier internalization and drug-release response ([44] and [17]). For example, 20 μg/mL of PLA (~900 nm) was reported to change the size of HT29 cells (indicating internalization) but did not affect cell viability or cell migration capacity [22]. PLA-NPLs as well as PLGA-NPLs were seen to have a high adhesive capacity in HT29-MTX cells, which might be a mucin-drive process [34]. On the other hand, cell uptake studies of PLA-NPLs demonstrated that Caco-2 cells are able to (1) internalize particles up to 2000 nm, (2) that positively charged PLA increases cell internalization, (3) that PLA internalization is ruled by multiple endocytosis pathways (*e.g.*, clathrin- and raft-dependent), and (4) that PLA-MPLs uptake is also temperature-dependent [14,16,27]. In other epithelial cells such as A549, da Luz and co-workers also stated that ~70 nm PLA-NPLs (2–200 μg/mL) uptake was mostly driven by clathrin-dependent mechanisms with lipid raft involvement [12]. All this together could suggest that since the HT29 cell clone (goblet-like cells) has the capability to secret higher content of mucus in the extracellular matrix, as compared to Caco-2 cells which are enterocyte-like cells, PLA-NPLs would get entrapped in the matrix having HT29 cells higher chances of encountering this type of NPLs.

3.5. *Effects of PLA-NPLs in the in vitro model of the intestinal barrier (Caco-2/HT29 cells)*

Once ingested, PLA-NPLs will eventually arrive in the small intestine. Physiologically, the small intestine (SI) is found coiled inside the lower portion of the abdominal cavity, sitting beneath the stomach, and framed by the large intestine. Functionally, SI oversees breaking down food (the last steps of stomach digestion), absorbing nutrients and minerals needed for the body, and getting rid of unnecessary components. However, SI plays a crucial role in the immune system, acting as a main barrier to a wide range of exogenous and endogenous substances and microorganisms making sure that no pathogen enters the inner parts of the body [10]. Due to the high complexity of the SI epithelium, this work has used a simple but physiologically relevant *in vitro* model (Caco-2/HT29) to investigate the PLA-NPLs' fate and biodistribution in the intestinal barrier. The *in vitro* barrier containing differentiated Caco-2 (90%) and HT29 (10%) cells growing together for 21 days mimics the first epithelium directly in contact with the intestinal lumen, where they interact with the gastric bolus containing all the ingested and digested components (food and food contaminants such as MNPLs). Bredeck and collaborators from the Joint Research Center (European Commission) advocate for the implementation of a tiered testing strategy, in which monocultures can serve as a tool for high-throughput testing of MNPLs, followed by co-cultures that can be used to assess the potential of a systemic uptake and finally using organs-on-a-chip to provide more insights into relevant dosimetry [4]. In our previous studies, we have already highlighted the suitability of the present *in vitro* model of intestinal barrier to assessing the bio-interactions of metal oxide-NPs and MNPLs, as well as their putative toxic and genotoxic effects, and the detrimental effects on the barrier structure and functionality [15,21]. All this background has been applied to successfully determine the interaction of PLA-NPLs with the *in vitro* model of the intestinal barrier.

Thus, after exposing Caco-2/HT29 barriers to teabag-derived PLA-NPLs, the flow cytometry analysis revealed that after 24 h the entire cell population (100%) interacted/internalized at least 1 teabag-derived particle (Fig. 6. D). Although confocal microscopy has less resolution detecting or showing the smaller particles (usually those in the nano range), it was possible to confirm that PLA-NPLs agglomerates were mostly internalized in the barrier (Fig. 6. A, B, and C), and these internalizations were seen to bio-persist after 72 h of exposure (Fig. 6. C). As mentioned, little is known about the tissue distribution and barrier internalization/translocation of pristine and surfactant-free PLA-NPLs. Recently, Paul and collaborators exposed an inflamed Caco-2-based *in vitro* model to 2000 nm and 250 nm PLA-NPLs for a period of 24 h. The study demonstrated that smaller PLA-NPLs (250 nm) could interact and be transported more than bigger particles (2000 nm); however, no differences were detected between healthy and inflamed (spiked with LPS) models [32]. In the study of McClean and colleagues, the binding, uptake, and absorption of different sizes of PLA-MNPLs in Caco-2 monolayers were determined, as well as in the ileal and gut-associated lymphoid tissues of rats and rabbits. Their investigation concluded that a total of 10% of MNPLs were adsorbed, being NPLs better absorbed than MPLs [27]. An interesting work by Tan et al. [37], demonstrated that only the hydrophilic block polymer PLA-PEG, modified with cell-penetrating peptide (achieving electroneutrality), reduced the mucus trapping by 36% and increased the cellular uptake by 2.3-folds. The transport capability of mPEG-PLGA-NPs across Caco-2/HT29-MTX barriers was higher than coating-free PLGA-NPs, suggesting that PEG coating could shield the surface charge and enhance the hydrophilicity of PLGA nanoparticles, which leads to higher anti-adhesion activity [42].

The high affinity for mucus-secreting cells could be triggered by different factors contributing to enhancing the particle permeation through a mucus matrix including the hydrophilicity of the polymer, the mucin content, and compactness, the particle size, as well as the cohesive and repulsive electrostatic forces between the mucins and particles. Like the work of Tan et al. [37], our particles achieved an almost electroneutrality when diluted in DMEM+ 10%FBS (-5.95 ± 1.88 mV) in comparison to when they were suspended in water (-34.30 ± 2.52 mV). Together with its small diameter size in DMEM (116 nm) the electroneutrality can grant the affinity for muco-substances and cellular internalization, consequently. Abdelkarim and co-workers already reported a meaningful relationship between particle diffusion in mucus, particle size, and particle surface charge, where the beneficial characteristic promoting diffusion was a neutral or near-neutral charge [1].

Despite the high cell interaction and uptake, teabags-derived PLA-NPLs were not seen to cause major cytotoxic nor structural damage in Caco-2/HT29 barriers after short-term exposures (up to 48 h). No significant differences were observed in cell viability after exposing both monocultures of undifferentiated Caco-2 and undifferentiated HT29 cells to 100 μg/mL of teabags-derived PLA-NPLs (Fig. 1. Supplementary Information). It is known that undifferentiated cells can be more susceptible to nanoparticles than differentiated barriers since they have developed more complex structures such as microvilli [40]. In the same way, no significant increments in the production of intracellular reactive oxygen species were observed when Caco-2/HT29 barriers were exposed to 50 and 100 μg/mL of teabag-derived PLA-NPLs, as reported

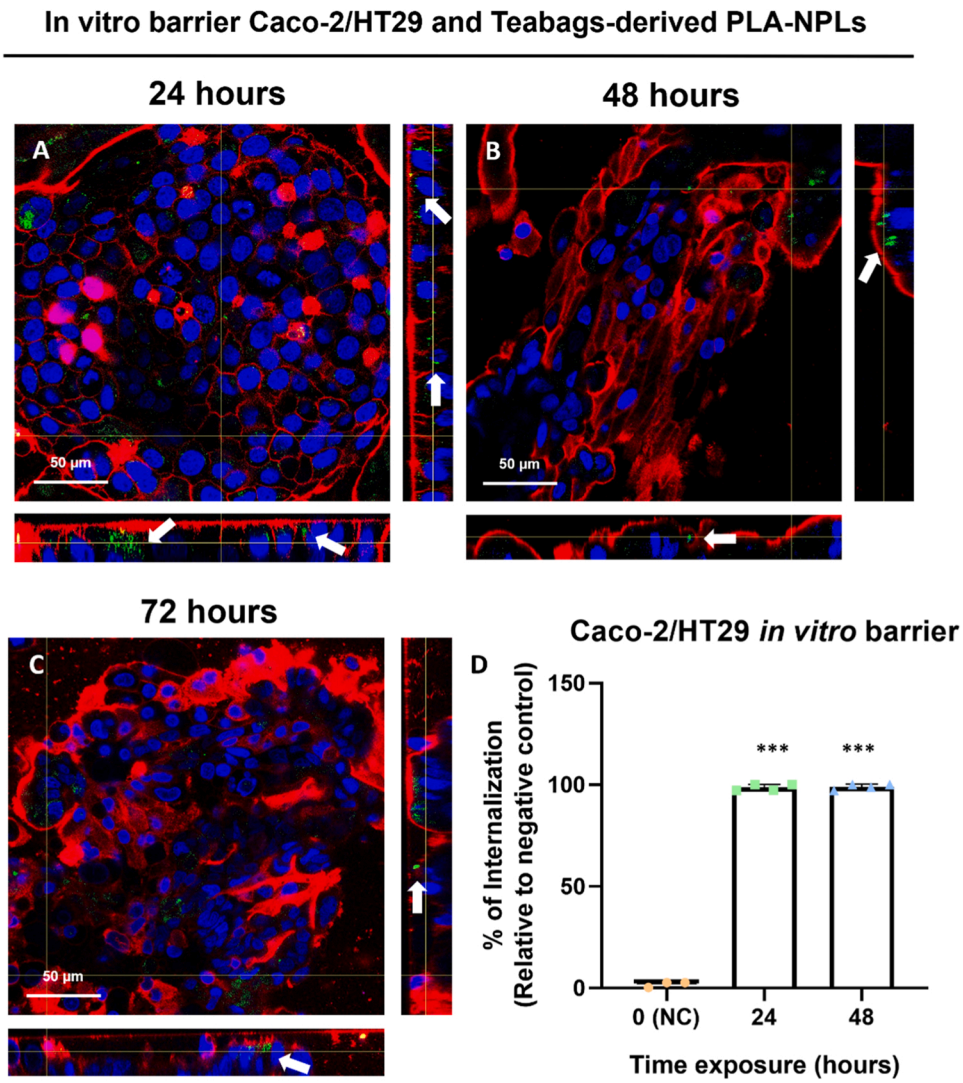

Fig. 6. Internalization studies in the *in vitro* model of Caco-2/HT29 barrier. (A, B, and C) Confocal images of differentiated barriers of Caco-2-HT29 cocultures exposed to 100 µg/mL teabags' PLA-NPLs for 24, 48, and 72 h, respectively. (D) Cell uptake quantification by flow cytometry of PLA-NPLs. PLA-NPLs (green), nuclei (blue), and cell membrane (red) were stained with iDYE, Hoechst 33342, and CellMask™, respectively. White arrows indicate PLA-NPLs internalization. Data is represented as mean ± SEM and analysed using one-way ANOVA with Dunett's post-test. * ** $P < 0.0001$.

in Fig. 7.A.

Studies testing the effects of pristine and free-coating PLA-NPLs were also performed using different *in vitro* models. Thus, Da Silva et al. [13] observed that small PLA-NPLs (~75 nm *vs* ~162 nm) reduced the viability of RAW 264.7 cells and increased ROS production. However, no detrimental effects were seen on PBMCs despite using high concentrations (up to 500 µg/mL). Other types of cells such as lung epithelial A549 also were used to detect PLA-NPLs (80–100 nm) internalization without observing toxicity or secretion of pro-inflammatory mediators [12]. Non-mammalian *in vivo* models have also been used to detect PLA-NPLs effects. Thus, Legaz et al. [25] observed that high doses of PLA-NPLs (500 µg/mL) reduce the larvae viability and, in the zebrafish 70 nm PLA-NPLs could internalize endothelial cells as well as macrophages after intravenous administration [33].

To study whether PLA-NPLs can disrupt the structure and functionality of the small intestine epithelium, two widely known assays were used to measure the integrity (TEER) and permeability (LY passage) of the *in vitro* barriers. The obtained TEER values (Fig. 7. B) indicate a slight but significant decrease in the barrier integrity after 3 h of PLA-NPLs exposure to both 50 and 100 µg/mL. However, this effect was not observed at extended exposures (24 and 48 h). Is worth mentioning that this is a one-time treatment, and although Caco-2 stops dividing when in confluency, HT29 slightly continues dividing. This could repair the initial damage by epithelium renewal and recover the initial TEER values. In real life, exposure to teabags-derived NPLs is repeated daily and in some cases several times a day, which could constantly compromise the gut epithelium.

Our results disagree with McClean's and colleague's work, where PLA-MNPLs (up to 10^7 particles/mL) did not affect TEER values of Caco-2 monolayers after 2 h of exposure. Is worth mentioning that they only detected 10% of particle adsorption [27]. When the content of LY (a molecule that only crosses paracellularly) is measured in the basolateral compartment, a slight tendency on increasing the paracellular transport is observed when increasing the PLA-NPLs concentration; but this increase did not attain statistical significance. Like this PLA-NPLs data, our previous results with 100 µg/mL polystyrene nanoplastics (PS-NPLs) did not disrupt the integrity nor the permeability of both systems, Caco-2/HT29 and Caco-2/HT29/Raji-b [15].

To emphasize the relevance and topicality of the discussed subject, two recent papers point out important questions such as the relationship between MNPLs exposure and inflammatory bowel disease [45], and the severe inflammation observed in the intestine and colon in mice exposed to PLA-MPLs under realistic human exposure doses [41]. In this last study, the observed inflammation was suggested to be probably induced by released oligomers, rather than by the direct particle fragments of PLA. This emphasizes the need of carrying out *in vitro* digestion studies to characterize their effects on PLA-MNPLs.

Although nanotoxicology is not a new field, the MNPLs sub-category has brought new challenges to researchers in toxicology. Some of the difficulties encountered, are i) the lack of information, as is a relatively

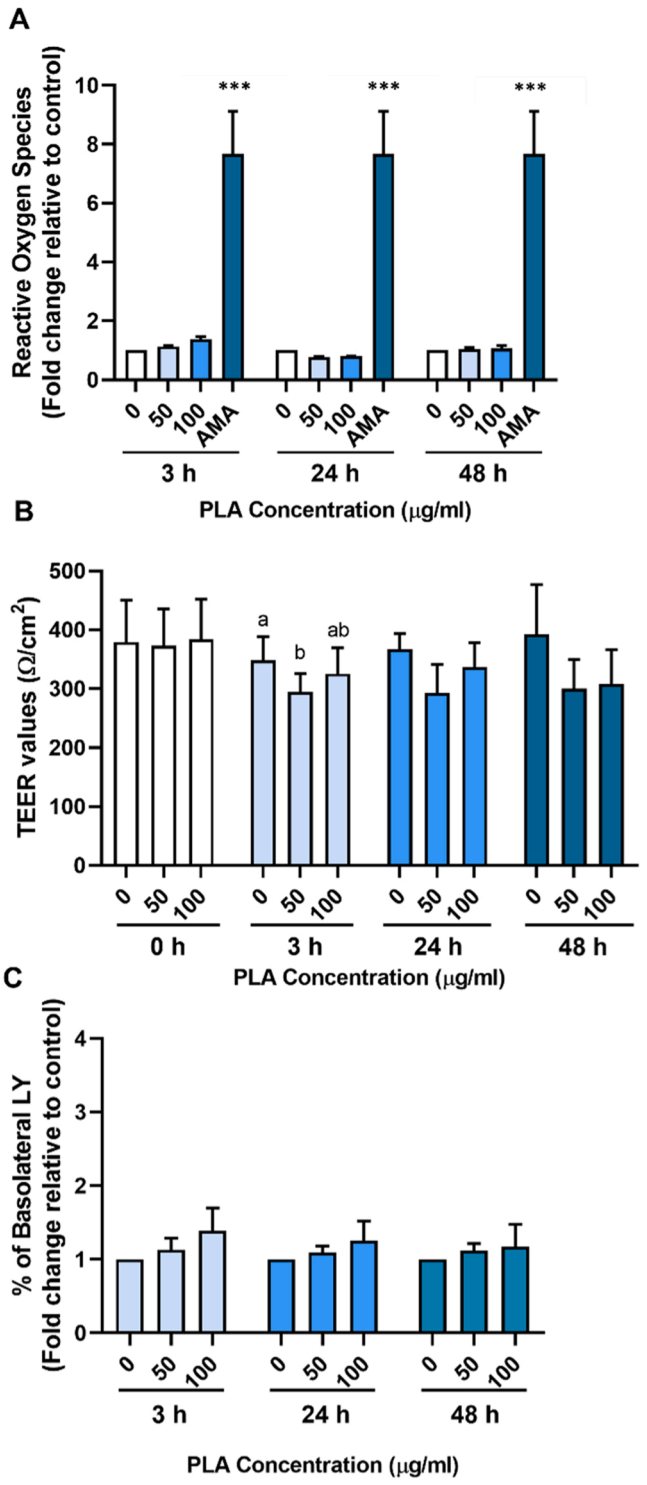

Fig. 7. Structural and functional studies on Caco-2/HT29 barriers. (A) Formation of intracellular reactive oxygen species after exposing Caco-2/HT29 barriers to 50 and 100 μg/mL teabags-derived PLA-NPLs for 48 h. Antimycin A (AMA) was used as the positive control. (B) TEER measurements after 0, 50, and 100 μg/mL teabags-derived PLA-NPLs treatments for up to 48 h. Those bars that do not share any letter are significantly different. (C) Percentage of basolateral LY after 0, 50, and 100 μg/mL teabags-derived PLA-NPLs treatments for up to 48 h. Data is represented as mean±SEM and analysed using the one-way ANOVA with Dunnett's post-test. * ** $P < 0.001$.

new subject; ii) the lack of reference materials to work in the laboratory; iii) as well as the need to adapt the existent techniques for polymer detection and quantification. In this framework, the present work is one of the few studies addressing the effects of pristine and free-coating PLA-NPLs and most important utilizing true-to-life NPLs (NPLs proceeding from real samples) for its hazard evaluation. We have overcome setbacks such as the use of high throughput extraction methods to obtain enough sample (and sterilized) for toxicological experiments and the use of appropriate staining to track the PLA-NPLs journey clearly and rapidly along the *in vitro* intestinal barrier.

4. Conclusions

This is the first time that a study uses true-to-life NPLs derived from teabags (specifically PLA-NPLs) to investigate their biodistribution, fate, and toxic effects using an *in vitro* model (Caco-2/HT29 coculture) that closely mimics the physiology of the small intestine epithelium. After an exhaustive characterization, we have demonstrated that teabags purchased in a local supermarket contained and released nanoplastics of polylactic acid, a well-known biodegradable polymer. These PLA-NPLs presented a spherical shape, a primary particle diameter of 160 nm, and a hydrodynamic size somewhere between 200 and 400 nm depending on the technique used to measure, NTA or DLS, respectively. The overall content of particles measured after the extraction was around 1×10^8 from a single teabag, which increased up to 8×10^8 (almost an order of magnitude higher) if the solution was dispersed by sonication suggesting that PLA-NPLs agglomerates can be separated. However, if only those particles were present in the range of the PLA primary particle size (~ 160 nm), the number of particles decreased by two orders of magnitude (8×10^6 particles per teabag). Afterward, we used those teabags-derived PLA-NPLs to study their potentially harmful effects *in vitro*. We concluded that: (i) PLA-NPLs can easily and rapidly internalize into gut-derived cells; (ii) mucins could play an important role in the adhesion; adsorption and retention of PLA particles since HT29 cells presented higher affinity; (iii) no cytotoxic effects were observed up to 100 μg/mL when analyzing the cell viability or the intracellular ROS production; and (iv) no structural nor functional damage is triggered in the *in vitro* barrier after one-time exposure and despite the PLA-NPLs bio-persistence in the tissue. Despite the lack of evident damage in the *in vitro* barrier after short-term exposures to PLA-NPLs, the potential bio-persistence of such particles might be of high concern since the actual consumption of tea is daily and several times per day. Moreover, it is of special concern the interaction between PLA-NPLs and cell nucleus, which through repeated and long-term exposures could trigger some sort of DNA damage or stress response as previously demonstrated by our group [3]. It is worth mentioning that only a few or almost no studies have addressed the potential effects of pristine and free-coating PLA-NPLs when ingested. Hence, the present study is of high relevance and served to raise a vast number of new and important questions such as: (1) are mucins a real protective layer against polymeric material if they have high-adhesive capacity? (2) what are the effects of continued PLA-NPLs exposure on overall human health? (3) will PLA-NPLs degrade along the human digestion process? (4) what are the effects of the PLA-NPLs leachates or by-products in the gastrointestinal system?

Environmental implication

Environmental micro/nanoplastics (MNPLs) are of special concern and determining their potential risk is essential. The obtention/evaluation of MNPLs obtained from teabags looks relevant due to their worldwide use. Interestingly, the component of the commercial brand used was polylactic acid (PLA) which constitutes one of the new eco-friendly plastic materials. Their increased environmental presence requires further efforts to determine their ability to release MNPLs, and the estimation of their potential risk. From this point of view, and as a

novelty, our study includes data on the interaction of PLA-MNPLs with an in vitro model of the intestinal barrier.

Author contribution statement

RM and AH planned the experiments. GB, AGR, AV, AT, and JMP carried out the experimental part. GB and AGR analyzed the data, carried out the statistical analysis, and prepared tables/figures. AGR, RM, and AH wrote the final manuscript.

CRediT authorship contribution statement

RM and AH planned the experiments. GB, AGR, AV, AT, and JMP carried out the experimental part. GB and AGR analyzed the data, carried out the statistical analysis, and prepared tables/figures. AGR, RM, and AH wrote the final manuscript.

Declaration of Competing Interest

The authors declare that they have no known competing financial interests or personal relationships that could have appeared to influence the work reported in this paper.

Acknowledgments

A. García-Rodríguez received funding from the postdoctoral fellowship program Beatriu de Pinós, funded by the Secretary of Universities and Research [Government of Catalonia] and by the Horizon 2020 program of Research and Innovation of the European Union under the Marie Sktodowsdka-Curie grant agreement No 801370. A. Villacorta was supported by Ph.D. fellowships from the National Agency for Research and Development (ANID), from the CONICYT PFCHA/DOCTORADO BECAS CHILE/2020–72210237. A Tavakolpournegari and J. Martin-P é rez hold Ph.D. fellowships from the Generalitat de Catalunya. A. Hernández was granted an ICREA ACADEMIA award.

This project has received funding from the European Union's Horizon 2020 Research and Innovation Program under Grant Agreement No. 965196. This work was also partially supported by the Spanish Ministry of Science and Innovation [PID2020-116789, RB-C43] and by the Generalitat de Catalunya (2021-SGR-00731).

Appendix A. Supporting information

Supplementary data associated with this article can be found in the online version at doi:10.1016/j.jhazmat.2023.131899.

References

[1] Abdulkarim, M., Agulló, N., Cattoz, B., Griffiths, P., Bernkop-Schnürch, A., Borros, S.G., et al., 2015. Nanoparticle diffusion within intestinal mucus: three-dimensional response analysis dissecting the impact of particle surface charge, size and heterogeneity across polyelectrolyte, pegylated and viral particles. Eur J Pharm Biopharm 97 (Pt A), 230–238. https://doi.org/10.1016/j.ejpb.2015.01.023.

[2] Afrin, S., Rahman, M.M., Akbor, M.A., Siddique, M.A.B., Uddin, M.K., Malafaia, G., 2022. Is there tea complemented with the appealing flavor of microplastics? a pioneering study on plastic pollution in commercially available tea bags in Bangladesh. Sci Total Environ 837, 155833. https://doi.org/10.1016/j.scitotenv.2022.155833.

[3] Barguilla, I., Domenech, J., Ballesteros, S., Rubio, L., Marcos, R., Hernández, A., 2022. Long-term exposure to nanoplastics alters molecular and functional traits related to the carcinogenic process. J Hazard Mater 438, 129470. https://doi.org/10.1016/j.jhazmat.2022.129470.

[4] Bredeck, G., Halamoda-Kenzaoui, B., Bogni, A., Lipsa, D., Bremer-Hoffmann, S., 2022. Tiered testing of micro- and nanoplastics using intestinal *in vitro* models to support hazard assessments. Environ Int 158, 106921. https://doi.org/10.1016/j.envint.2021.106921.

[5] Busse, K., Ebner, I., Humpf, H.U., Ivleva, N., Kaeppler, A., Oßmann, B.E., et al., 2020. Comment on plastic teabags release billions of microparticles and nanoparticles into tea. Environ Sci Technol 54 (21), 14134–14135. https://doi.org/10.1021/acs.est.0c03182.

[6] Castro-Aguirre, E., Iñiguez-Franco, F., Samsudin, H., Fang, X., Auras, R., 2016. Poly (lactic acid) mass production, processing industrial applications and end of life. Adv Drug Deliv Rev 107, 333–366. https://doi.org/10.1016/j.addr.2016.03.010.

[7] Cella, C., La Spina, R., Mehn, D., Fumagalli, F., Ceccone, G., Valsesia, A., et al., 2022. Detecting micro- and nanoplastics released from food packaging: challenges and analytical strategies. Polymers 14 (6), 1238. https://doi.org/10.3390/polym14061238.

[8] Chieng, B.W., Ibrahim, N.A., Yunus, W.M.Z.W., Hussein, M.Z., 2014. Poly(lactic acid)/poly(ethylene glycol) polymer nanocomposites: effects of graphene nanoplatelets. Polymers 6, 93–104. https://doi.org/10.3390/polym6010093.

[9] Chou, S.H., Chuang, Y.K., Lee, C.M., Chang, Y.S., Jhang, Y.J., Yeh, C.W., et al., 2022. and (Semi-)quantification of submicrometer plastics through scanning electron microscopy and time-of-flight secondary ion mass spectrometry. Environ Pollut 300, 118964. https://doi.org/10.1016/j.envpol.2022.118964.

[10] Collins J.T., Nguyen A., Badireddy M. Anatomy, abdomen and pelvis, small intestine. In: StatPearls [Internet]. Treasure Island (FL): StatPearls Publishing; 2023 Jan–. PMID: 29083773.

[11] Courtene-Jones, W., Clark, N.J., Thompson, R.C., 2022. Plastic pollution: the science we need for the planet we want. Emerg Top Life Sci 6 (4), 333–337. https://doi.org/10.1042/ETLS20220019.

[12] da Luz, C.M., Boyles, M.S., Falagan-Lotsch, P., Pereira, M.R., Tutumi, H.R., de Oliveira Santos, E., et al., 2017. Poly-lactic acid nanoparticles (PLA-NP) promote physiological modifications in lung epithelial cells and are internalized by clathrin-coated pits and lipid rafts. J Nanobiotechnol 15 (1), 11. https://doi.org/10.1186/s12951-016-0238-1.

[13] Da Silva, J., Jesus, S., Bernardi, N., Colaço, M., Borges, O., 2019. Poly(D,L-lactic acid) nanoparticle size reduction increases its immunotoxicity. Front Bioeng Biotechnol 7, 137. https://doi.org/10.3389/fbioe.2019.00137.

[14] Desai, M.P., Labhasetwar, V., Walter, E., Levy, R.J., Amidon, G.L., 1997. The mechanism of uptake of biodegradable microparticles in Caco-2 cells is size dependent. Pharm Res 14 (11), 1568–1573. https://doi.org/10.1023/a:1012126301290.

[15] Domenech, J., Hernández, A., Rubio, L., Marcos, R., Cortés, C., 2020. Interactions of polystyrene nanoplastics with *in vitro* models of the human intestinal barrier. Arch Toxicol 94 (9), 2997–3012. https://doi.org/10.1007/s00204-020-02805-3.

[16] Du, X.J., Wang, J.L., Iqbal, S., Li, H.J., Cao, Z.T., Wang, Y.C., et al., 2018. The effect of surface charge on oral absorption of polymeric nanoparticles. Biomater Sci 6 (3), 642–650. https://doi.org/10.1039/c7bm01096f.

[17] Essa, D., Kondiah, P.P.D., Choonara, Y.E., Pillay, V., 2020. The design of poly (lactide-co-glycolide) nanocarriers for medical applications. Front Bioeng Biotechnol 8, 48. https://doi.org/10.3389/fbioe.2020.00048.

[18] Foetisch, A., Filella, M., Watts, B., Vinot, L.H., Bigalke, M., 2022. Identification and characterisation of individual nanoplastics by scanning transmission X-ray microscopy (STXM). J Hazard Mater 426, 127804. https://doi.org/10.1016/j.jhazmat.2021.127804.

[19] García-Rodríguez, A., Vila, L., Cortés, C., Hernández, A., Marcos, R., 2018. Exploring the usefulness of the complex *in vitro* intestinal epithelial model Caco-2/HT29/Raji-B in nanotoxicology. Food Chem Toxicol 113, 162–170. https://doi.org/10.1016/j.fct.2018.01.042.

[20] García-Rodríguez, A., Vila, L., Cortés, C., Hernández, A., Marcos, R., 2018. Effects of differently shaped TiO_2NPs (nanospheres, nanorods, and nanowires) on the *in vitro* model (Caco-2/HT29) of the intestinal barrier. Part Fibre Toxicol 15 (1), 33. https://doi.org/10.1186/s12989-018-0269-x.

[21] García-Rodríguez, A., Moreno-Olivas, F., Marcos, R., Tako, E., Marques, C.N.H., Mahler, G.J., 2020. The role of metal oxide nanoparticles, *Escherichia coli*, and *Lactobacillus rhamnosus* on small intestinal enzyme activity. Environ Sci Nano 7 (12), 3940–3964. https://doi.org/10.1039/d0en01001d.

[22] Helal-Neto, E., Barros, A.O.D.S., Saldanha-Gama, R., Brandão-Costa, R., Alencar, L.M.R., Santos, C.C.D., et al., 2019. Molecular and cellular risk assessment of healthy human cells and cancer human cells exposed to nanoparticles. Int J Mol Sci 21 (1), 230. https://doi.org/10.3390/ijms21010230.

[23] Hernandez, L.M., Xu, E.G., Larsson, H.C.E., Tahara, R., Maisuria, V.B., Tufenkji, N., 2019. Plastic teabags release billions of microparticles and nanoparticles into tea. Environ Sci Technol 53 (21), 12300–12310. https://doi.org/10.1021/acs.est.9b02540.

[24] Kniazev, K., Pavlovetc, I.M., Zhang, S., Kim, J., Stevenson, R.L., Doudrick, K., et al., 2021. Using infrared photothermal heterodyne imaging to characterize micro- and nanoplastics in complex environmental matrices. Environ Sci Technol 55 (23), 15891–15899. https://doi.org/10.1021/acs.est.1c05181.

[25] Legaz, S., Exposito, J.Y., Lethias, C., Viginier, B., Terzian, C., Verrier, B., 2016. Evaluation of polylactic acid nanoparticles safety using *Drosophila* model. Nanotoxicology 10 (8), 1136–1143. https://doi.org/10.1080/17435390.2016.1181806.

[26] Mateos-Cárdenas, A., 2022. Fate of petroleum-based and plant-based teabags exposed to environmental soil conditions for one year. Front Bioeng Biotechnol 10, 966685. https://doi.org/10.3389/fbioe.2022.966685.

[27] McClean, S., Prosser, E., Meehan, E., O'Malley, D., Clarke, N., Ramtoola, Z., et al., 1998. Binding and uptake of biodegradable poly-DL-lactide micro- and nanoparticles in intestinal epithelia. Eur J Pharm Sci 6 (2), 153–163. https://doi.org/10.1016/s0928-0987(97)10007-0.

[28] Mei, T., Wang, J., Xiao, X., Lv, J., Li, Q., Dai, H., et al., 2022. Identification and evaluation of microplastics from tea filter bags based on Raman imaging. Foods 11 (18), 2871. https://doi.org/10.3390/foods11182871.

[29] Meng, K., Teng, Y., Ren, W., Wang, B., Geissen, V., 2023. Degradation of commercial biodegradable plastics and temporal dynamics of associated bacterial

communities in soils: a microcosm study. Sci Total Environ 865, 161207. https://doi.org/10.1016/j.scitotenv.2022.161207.
[30] Meyers, N., Catarino, A.I., Declercq, A.M., Brenan, A., Devriese, L., Vandegehuchte, M., et al., 2022. Microplastic detection and identification by Nile red staining: towards a semi-automated cost- and time-effective technique. Sci Total Environ 823, 153441. https://doi.org/10.1016/j.scitotenv.2022.153441.
[31] Nanogenotox. 2011. ⟨http://www.nanogenotox.eu/files/PDF/Deliverables/nanogenotox%20deliverable%203_wp4_%20dispersion%20protocol.pdf⟩.
[32] Paul, M.B., Schlief, M., Daher, H., Braeuning, A., Sieg, H., Böhmert, L., 2023. A human Caco-2-based co-culture model of the inflamed intestinal mucosa for particle toxicity studies (Online ahead of print.). Vitr Models 1 (7). https://doi.org/10.1007/s44164-023-00047-y.
[33] Rességuier, J., Levraud, J.P., Dal, N.K., Fenaroli, F., Primard, C., Wohlmann, J., et al., 2021. Biodistribution of surfactant-free poly(lactic-acid) nanoparticles and uptake by endothelial cells and phagocytes in zebrafish: evidence for endothelium to macrophage transfer. J Control Release 331, 228–245. https://doi.org/10.1016/j.jconrel.2021.01.006.
[34] Roque, L., Alopaeus, J., Reis, C., Rijo, P., Molpeceres, J., Hagesaether, E., et al., 2018. Mucoadhesive assessment of different antifungal nanoformulations. Bioinspir Biomim 13 (5), 055001. https://doi.org/10.1088/1748-3190/aad488.
[35] Sewwandi, M., Wijesekara, H., Rajapaksha, A.U., Soysa, S., Vithanage, M., 2023. Microplastics and plastics-associated contaminants in food and beverages; global trends concentrations and human exposure. Environ Pollut 317, 120747. https://doi.org/10.1016/j.envpol.2022.120747.
[36] Swetha, T.A., Bora, A., Mohanrasu, K., Balaji, P., Raja, R., Ponnuchamy, K., et al., 2023. A comprehensive review on polylactic acid (PLA) -Synthesis processing and application in food packaging. Int J Biol Macromol 234, 123715. https://doi.org/10.1016/j.ijbiomac.2023.123715.
[37] Tan, X., Yin, N., Liu, Z., Sun, R., Gou, J., Yin, T., et al., 2020. Hydrophilic and electroneutral nanoparticles to overcome mucus trapping and enhance oral delivery of insulin. Mol Pharm 17 (9), 3177–3191. https://doi.org/10.1021/acs.molpharmaceut.0c00223.
[38] Tavakolpournegari, A., Annangi, B., Villacorta, A., Banaei, G., Martin, J., Pastor, S., et al., 2023. Hazard assessment of different-sized polystyrene nanoplastics in three hematopoietic human cell lines. Chemosphere 325, 138360. https://doi.org/10.1016/j.chemosphere.2023.138360.
[39] Vela, L., Villacorta, A., Venus, T., Estrela-Lopis, I., Pastor, S., García-Rodriguez, A., et al., 2023. The potential effects of *in vitro* digestion on the physicochemical and biological characteristics of polystyrene nanoplastics. Environ Pollut 329, 121656. https://doi.org/10.1016/j.envpol.2023.121656.
[40] Vila, L., García-Rodríguez, A., Cortés, C., Velázquez, A., Xamena, N., Sampayo-Reyes, A., et al., 2018. Effects of cerium oxide nanoparticles on differentiated/undifferentiated human intestinal Caco-2 cells. Chem Biol Interact 283, 38–46. https://doi.org/10.1016/j.cbi.2018.01.018.
[41] Wang, M., Li, Q., Shi, C., Lv, J., Xu, Y., Yang, J., et al., 2023. Oligomer nanoparticle release from polylactic acid plastics catalysed by gut enzymes triggers acute inflammation. Nat Nanotechnol 18 (4), 403–411. https://doi.org/10.1038/s41565-023-01329-y.
[42] Wen, Z., Li, G., Lin, D.H., Wang, J.T., Qin, L.F., Guo, G.P., 2013. Transport of PLGA nanoparticles across Caco-2/HT29-MTX co-cultured cells. Yao Xue Xue Bao 48 (12), 1829–1835.
[43] Xu, J.L., Lin, X., Hugelier, S., Herrero-Langreo, A., Gowen, A.A., 2021. Spectral imaging for characterization and detection of plastic substances in branded teabags. J Hazard Mater 418, 126328. https://doi.org/10.1016/j.jhazmat.2021.126328.
[44] Zhang, Z., Lee, S.H., Gan, C.W., Feng, S.S., 2008. *In vitro* and *in vivo* investigation on PLA-TPGS nanoparticles for controlled and sustained small molecule chemotherapy. Pharm Res 25 (8), 1925–1935. https://doi.org/10.1007/s11095-008-9611-6.
[45] Zhao, Y., Liu, S., Xu, H., 2023. Effects of microplastic and engineered nanomaterials on inflammatory bowel disease: a review. Chemosphere 326, 138486. https://doi.org/10.1016/j.chemosphere.
[46] Zhou, Y., Ashokkumar, V., Amobonye, A., Bhattacharjee, G., Sirohi, R., Singh, V., et al., 2023. Current research trends on cosmetic microplastic pollution and its impacts on the ecosystem: a review. Environ Pollut 320, 121106. https://doi.org/10.1016/j.envpol.2023.121106.